

# Variable Noninnocence of Substituted Azobis(phenylcyanamido)diruthenium Complexes

Mohammad M. R. Choudhuri,<sup>†</sup> Mahdi Behzad,<sup>‡</sup> Mousa Al-Noaimi,<sup>§</sup> Glenn P. A. Yap,<sup>⊥</sup> Wolfgang Kaim,<sup>||</sup> Biprajit Sarkar,<sup>||</sup> and Robert J. Crutchley<sup>\*,†</sup>

<sup>†</sup>Chemistry Department, Carleton University, Ottawa, Ontario K1S 5B6, Canada

<sup>‡</sup>Department of Chemistry, Semnan University, Semnan 35131-19111, Iran

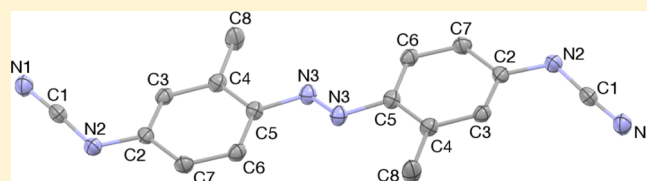
<sup>§</sup>Chemistry Department, Faculty of Science, The Hashemite University, Zarka 13115 Jordan

<sup>⊥</sup>Department of Chemistry & Biochemistry, University of Delaware, Newark, Delaware 19716, United States

<sup>||</sup>Institut für Anorganische Chemie, Universität Stuttgart, Pfaffenwaldring 55, Stuttgart D-70550, Germany

## Supporting Information

**ABSTRACT:** The synthetic chemistry of substituted 4,4'-azobis(phenylcyanamide) ligands was investigated, and the complexes  $[\{\text{Ru}(\text{tpy})(\text{bpy})\}_2(\mu\text{-L})][\text{PF}_6]_2$ , where  $\text{L} = 2,2':5,5'$ -tetramethyl-4,4'-azobis(phenylcyanamido) ( $\text{Me}_4\text{adpc}^{2-}$ ), 2,2'-dimethyl-4,4'-azobis(phenylcyanamido) ( $\text{Me}_2\text{adpc}^{2-}$ ), unsubstituted ( $\text{adpc}^{2-}$ ), 3,3'-dichloro-4,4'-azobis(phenylcyanamido) ( $\text{Cl}_2\text{adpc}^{2-}$ ), and 2,2':5,5'-tetrachloro-4,4'-azobis(phenylcyanamido) ( $\text{Cl}_4\text{adpc}^{2-}$ ), were prepared and characterized by cyclic voltammetry and vis–near-IR (NIR) and IR spectroelectrochemistry. The room temperature electron paramagnetic resonance spectrum of  $[\{\text{Ru}(\text{tpy})(\text{bpy})\}_2(\mu\text{-Me}_4\text{adpc})]^{3+}$  showed an organic radical signal and is consistent with an oxidation-state description  $[\text{Ru}^{\text{II}}, \text{Me}_4\text{adpc}^{\bullet-}, \text{Ru}^{\text{II}}]^{3+}$ , while that of  $[\{\text{Ru}(\text{tpy})(\text{bpy})\}_2(\mu\text{-Cl}_2\text{adpc})]^{3+}$  at 10 K showed a low-symmetry  $\text{Ru}^{\text{III}}$  signal, which is consistent with the description  $[\text{Ru}^{\text{III}}, \text{Cl}_2\text{adpc}^{2-}, \text{Ru}^{\text{II}}]^{3+}$ . IR spectroelectrochemistry data suggest that  $[\{\text{Ru}(\text{tpy})(\text{bpy})\}_2(\mu\text{-adpc})]^{3+}$  is delocalized and  $[\{\text{Ru}(\text{tpy})(\text{bpy})\}_2(\mu\text{-Cl}_2\text{adpc})]^{3+}$  and  $[\{\text{Ru}(\text{tpy})(\text{bpy})\}_2(\mu\text{-Cl}_4\text{adpc})]^{3+}$  are valence-trapped mixed-valence systems. A NIR absorption band that is unique to all  $[\{\text{Ru}(\text{tpy})(\text{bpy})\}_2(\mu\text{-L})]^{3+}$  complexes is observed; however, its energy and intensity vary depending on the nature of the bridging ligand and, hence, the complexes' oxidation-state description.



## INTRODUCTION

Studies of mixed-valence coordination complexes have played an important role in understanding electron transfer and confirming the Marcus–Hush theory.<sup>1</sup> These studies had immediate application to biological electron transfer,<sup>2</sup> but present day application is focused on the creation of novel electrooptic materials and molecular devices.<sup>3</sup> To achieve success in these applications, it is necessary to understand how mixed-valence properties can be expressed and controlled.

The vast majority of mixed-valence complexes are symmetric and are composed of electron-donor and -acceptor metal ions bridged by a polyatomic ligand. Because the metal ions are well separated, direct overlap of donor and acceptor wave functions is not possible and metal–metal coupling occurs through the superexchange mechanism using the bridging ligand orbitals.<sup>4</sup> For many types of bridging ligands, metal–metal coupling is often weak, and this gives rise to a valence-trapped mixed-valence state. However, if there is a good symmetry and energy match between donor and acceptor wave functions and the bridging ligand orbitals, strong metal–metal coupling can result in the formation of a delocalized state in which the odd electron is shared equally between metal ions. Electron-transfer or hole-transfer superexchange can occur using the bridging ligand empty or filled orbitals, respectively. In the case of hole-transfer

superexchange, the mixing of the acceptor wave function with the bridging ligand highest occupied molecular orbital (HOMO) effectively extends the acceptor wave function onto the bridging ligand. It is then possible to conceive of a situation in which the acceptor wave function is entirely on the bridging ligand (i.e., the ligand is oxidized) and the noninnocence of the bridging ligand is realized. The spectroscopic consequence of this transition from valence-trapped, delocalized to a non-innocent state has not been previously examined to our knowledge.

In past research, it was shown that  $\pi$  interactions between donor–acceptor–donor groups, NCN–diphenylazo–NCN, of the bridging ligand 4,4'-azobis(phenylcyanamide) dianion ( $\text{adpc}^{2-}$ ) created a continuous  $\pi$ -superexchange pathway that spanned the entire ligand.<sup>5,6</sup>

The planarity of this bridging ligand was confirmed in a crystal structure of  $[\{\text{Ru}(\text{tpy})(\text{bpy})\}_2(\mu\text{-adpc})][\text{PF}_6]_2$ , where tpy is 2,2':6',2''-terpyridine and bpy is 2,2'-bipyridine.<sup>5</sup> Electrochemical and spectroscopic studies of the mixed-valence complex  $[\{\text{Ru}(\text{tpy})(\text{bpy})\}_2(\mu\text{-adpc})]^{3+}$  were consistent with a delocalized case or a class III system in the Robin and Day

Received: October 10, 2014

classification,<sup>7</sup> having a large comproportionation constant  $K_c = 10^{13}$  and a low-energy near-IR (NIR) band centered at 1920 nm ( $\epsilon = 6000 \text{ M}^{-1} \text{ cm}^{-1}$ ) in *N,N*-dimethylformamide (DMF). Hartree–Fock calculations of free  $\text{adpc}^{2-}$  showed that both HOMO and lowest unoccupied molecular orbital (LUMO) of  $\text{adpc}^{2-}$  provided a pathway for hole- and electron-transfer superexchange, respectively.<sup>5</sup>

In a later study,<sup>8</sup> gas-phase density functional theory (DFT) calculations of  $[\{\text{Ru}(\text{tpy})(\text{bpy})\}_2(\mu\text{-adpc})]^{3+}$  were consistent with a ligand-centered radical species  $[\text{Ru}^{\text{II}}, \text{adpc}^{\bullet-}, \text{Ru}^{\text{III}}]^{3+}$  and, if correct, this would require reinterpretation of the complex's electrochemical and spectroscopic data. However, DFT calculations of noninnocent systems, while excellent in most cases,<sup>9</sup> are not always reliable because of the limits of the method and, in particular, inadequate modeling of solvent perturbations. For example, in a recent study,<sup>10</sup> electron paramagnetic resonance (EPR) spectroscopy unambiguously assigned the oxidation-state description  $[\text{Ru}^{\text{II}}, \text{dicyd}^{2-}, \text{Ru}^{\text{III}}]^{3+}$  to the mixed-valence complex,  $[\{\text{Ru}(\text{NH}_3)_5\}_2(\mu\text{-dicyd})]^{3+}$ , where  $\text{dicyd}^{2-}$  is a 1,4-dicyanamidobenzene dianion, even though gas-phase DFT calculations supported the dicyd radical anion description,  $[\text{Ru}^{\text{II}}, \text{dicyd}^{\bullet-}, \text{Ru}^{\text{III}}]^{3+}$ . DFT calculations on this molecule could only be reconciled with experimental results when specific solvent–solute donor–acceptor interactions were incorporated in the model.

An EPR study of  $[\{\text{Ru}(\text{tpy})(\text{bpy})\}_2(\mu\text{-adpc})]^{3+}$  would have been expected to provide substantive proof of this complex's oxidation-state description. Unfortunately, we were unable to observe an EPR signal of this complex in DMF down to liquid-helium temperatures. Although this apparently rapid (enhanced) EPR relaxation can be traced to significant participation of a heavy metal with a high spin–orbit coupling constant to the singly occupied molecular orbital (SOMO), thus indirectly suggesting a metal-based spin, we, nevertheless, decided to synthesize a series of substituted  $\text{adpc}^{2-}$  ligands, which when incorporated into a mixed-valence complex, should provide a range of properties that would be sufficient to establish an oxidation-state description.

This study reports the syntheses of substituted azobis(phenylcyanamide) ligands  $\text{R}_2\text{R}'_2\text{-adpc}^{2-}$  (Figure 1). In

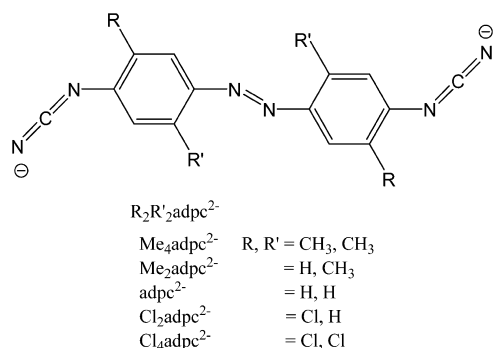


**Figure 1.** Substituted 4,4'-azobis(phenylcyanamide) dianion ( $\text{R}_2\text{R}'_2\text{-adpc}^{2-}$ ) ligands.

addition, the complexes  $[\{\text{Ru}(\text{tpy})(\text{bpy})\}_2(\mu\text{-R}_2\text{R}'_2\text{adpc})][\text{PF}_6]_2$  were prepared and characterized by cyclic voltammetry (CV), vis-NIR and IR spectroelectrochemistry, and EPR spectroscopy. EPR spectroscopy showed an organic radical signal for  $[\{\text{Ru}(\text{tpy})(\text{bpy})\}_2(\mu\text{-Me}_4\text{adpc})]^{3+}$  and an axial  $\text{Ru}^{\text{III}}$  signal for  $[\{\text{Ru}(\text{tpy})(\text{bpy})\}_2(\mu\text{-Cl}_2\text{adpc})]^{3+}$ . This study, there-

fore, reveals a transition between oxidation-state descriptions for these noninnocent systems.

## RESULTS AND DISCUSSION

**Synthesis.** Only 4,4'-azodianiline is available commercially albeit at significant expense, and because of this, the syntheses of substituted azodianiline derivatives were investigated. These are described in the Supporting Information (SI).

Preparation of the substituted 4,4'-azobis(phenylcyanamide) ligands required three different procedures from the corresponding azodianilines (Schemes 1–3). Method 1 (Scheme 1) proved to be the most dependable route to azobis(phenylcyanamide)s, giving relatively modest yields of 50–55%, while method 2 (Scheme 2) gave nearly quantitative yields (95%) for the preparation of  $\text{Me}_2\text{adpcH}_2$  and unsubstituted  $\text{adpcH}_2$ . Methods 2 and 3 (Scheme 3) gave a trace or no yield at all for chlorinated azodianilines, and this was probably due to deactivation of the amines by the chlorinated arene groups. The synthesis of  $\text{Cl}_4\text{adpcH}_2$  could only be achieved following Scheme 1 but with poor purity.

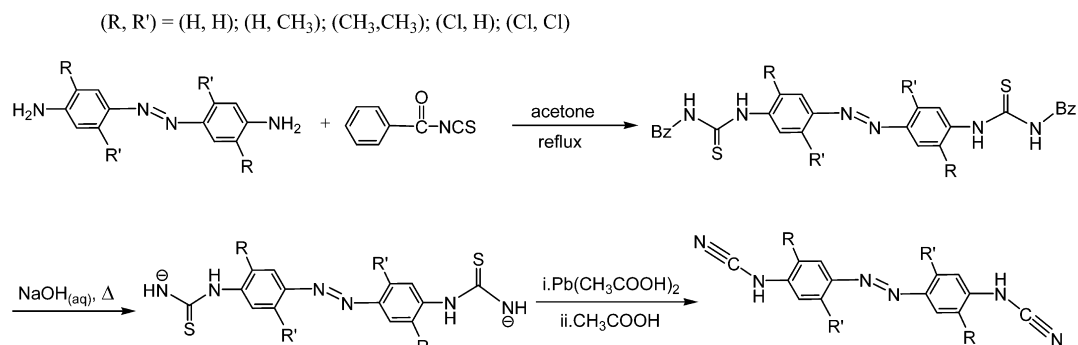
Thallium salts of  $\text{Cl}_2\text{adpc}^{2-}$  and  $\text{Me}_2\text{adpc}^{2-}$  were prepared following the published procedure<sup>5</sup> for  $\text{Tl}_2[\text{adpc}]$  and gave good elemental analyses. However,  $\text{Tl}_2[\text{Cl}_4\text{adpc}]$  could not be prepared in high purity, and all attempts to make the  $\text{Tl}^+$  or  $[\text{AsPh}_4]^+$  salt of  $\text{Me}_4\text{adpc}^{2-}$  were unsuccessful.

The  $[\{\text{Ru}(\text{tpy})(\text{bpy})\}_2(\mu\text{-L})][\text{PF}_6]_2$  complexes, where L is  $\text{Me}_2\text{adpc}^{2-}$ ,  $\text{adpc}^{2-}$ ,  $\text{Cl}_2\text{adpc}^{2-}$ , and  $\text{Cl}_4\text{adpc}^{2-}$ , were prepared by the salt metathesis reaction of  $[\text{Ru}(\text{tpy})(\text{bpy})\text{Cl}][\text{PF}_6]$  with  $\text{Tl}_2[\text{L}]$  in refluxing DMF, under argon. The ligand substitution reaction of  $\text{Me}_4\text{adpc}^{2-}$ , prepared by deprotonation of the neutral ligand with butyllithium, with 2 equiv of the solvato complex  $[\text{Ru}(\text{tpy})(\text{bpy})(\text{DMF})]^{2+}$ , prepared in situ by adding TlPF<sub>6</sub> to  $[\text{Ru}(\text{tpy})(\text{bpy})\text{Cl}][\text{PF}_6]$ , yielded  $[\{\text{Ru}(\text{tpy})(\text{bpy})\}_2(\mu\text{-Me}_4\text{adpc})][\text{PF}_6]_2$ . Recrystallization of  $[\{\text{Ru}(\text{tpy})(\text{bpy})\}_2(\mu\text{-Me}_2\text{adpc})][\text{PF}_6]_2$  resulted in good purity and high yields of ~90%. The other complexes required column chromatography, and the final yields of pure complexes were 30–40%. The complexes were air-stable, and acetonitrile and DMF solutions of the complexes remained unchanged for several days after preparation.

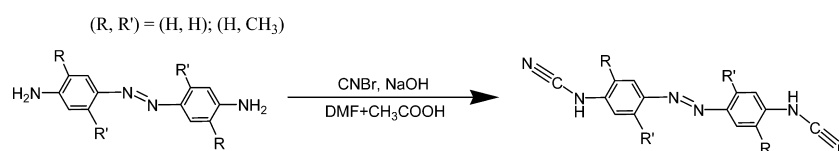
**NMR Spectroscopy.** The <sup>1</sup>H NMR spectra of the complexes  $\text{R}_2\text{R}'_2\text{adpcH}_2$  and  $\text{Tl}_2[\text{R}_2\text{R}'_2\text{adpc}]$  salts in dimethyl sulfoxide ( $\text{DMSO}-d_6$ ) were obtained, and the data are placed in the SI (Tables S1–S3). For all dinuclear complexes, a total of 14 peaks were observed in the region between 9.70 and 7.15 ppm for tpy and bpy protons, while the signals from the protons on the bridging  $\text{adpc}^{2-}$  ligand appear in the region between 7.20 and 5.65 ppm. Integration confirms that the complexes are symmetrical dinuclear systems. An unambiguous assignment of tpy and bpy protons as well as those on  $\text{adpc}^{2-}$  ligands was possible using a 2D COSY technique in combination with the observed splitting pattern and corresponding *J* values (Figure S13 in the SI).

**X-ray Crystallography.** The X-ray crystal structure of  $[\{\text{Ru}(\text{tpy})(\text{bpy})\}_2(\mu\text{-adpc})][\text{PF}_6]_2$  has been previously published<sup>5</sup> and shows that the  $\text{Ru}^{2+}$  ion occupies the pseudooctahedral coordination sphere of nitrogen donor atoms and that the  $\text{adpc}^{2-}$  ligand is approximately planar with two cyanamide groups in an anti conformation and the azo group in a trans conformation. We were interested to see if substituents ortho to the azo group might induce the bridging ligand to adopt a nonplanar geometry. Good-quality crystals of  $[\{\text{Ru}(\text{tpy})(\text{bpy})\}_2(\mu\text{-L})][\text{PF}_6]_2$ , where L =  $\text{Cl}_4\text{adpc}^{2-}$ ,

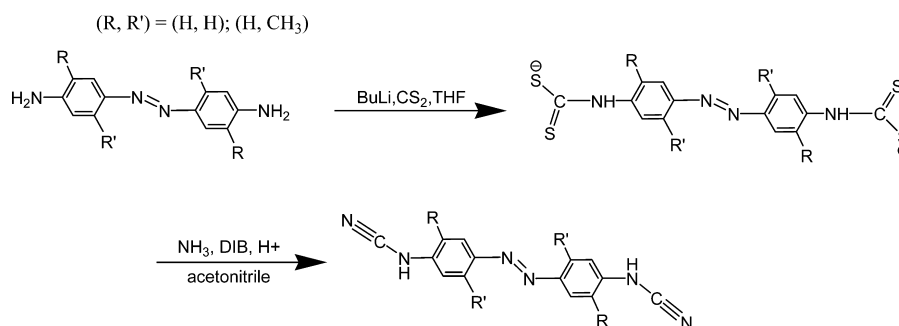
## Scheme 1. Method 1



## Scheme 2. Method 2



## Scheme 3. Method 3



Cl<sub>2</sub>adpc<sup>2-</sup>, Me<sub>2</sub>adpc<sup>2-</sup>, and Me<sub>4</sub>adpc<sup>2-</sup>, could not be grown. Nevertheless, suitable yellow-orange crystals of the tetraphenylarsonium salt of 2,2'-dimethyl-4,4'-azobis(phenylcyanamide) were grown from a boiling mixture of acetone and water (2:1). Crystallography data and bond lengths and angles have been placed in the SI (Tables S4–S9). An ORTEP drawing of the Me<sub>2</sub>adpc<sup>2-</sup> ion is shown in Figure S14 in the SI and shows that the planarity of Me<sub>2</sub>adpc<sup>2-</sup> is retained even in the presence of two methyl groups ortho to the azo group.

### ELECTRONIC ABSORPTION SPECTROSCOPY

The electronic absorption data of the thallium salts of anionic ligands, dinuclear complexes, and their oxidized products in DMF are compiled in Table 1. Assignments are based on previous studies.<sup>5,11</sup> All free R<sub>2</sub>R<sub>2'</sub>adpc<sup>2-</sup> ions show an intense absorption at 500–550 nm, which can be assigned to cyanamide-to-azo intramolecular charge-transfer (ICT) transitions. The dinuclear [ $\{\text{Ru}(\text{tpy})(\text{bpy})\}_2(\mu\text{-R}_2\text{R}_2'\text{adpc})\]^{2+}$  complexes show the same ICT transition as well as intense metal-to-ligand charge-transfer (MLCT) transitions for Ru<sup>II</sup>-to-tpy and -bpy chromophores in the same spectral region.

**Electrochemistry.** The CV data for the dinuclear complexes in acetonitrile and the thallium salts of ligands in DMF are shown in Table 2. The CV data for the mononuclear complex [Ru(tpy)(bpy)(2,4-Cl<sub>2</sub>pcyd)][PF<sub>6</sub>] are also included

here for comparison.<sup>11</sup> The voltammograms of the thallium salts of anionic ligands R<sub>2</sub>R<sub>2'</sub>adpc<sup>2-</sup> in DMF showed two closely spaced oxidation waves in the region between 0.3 and 0.7 V vs NHE, and both couples were shifted to positive potentials when electron-donating methyl substituents were replaced by chloro substituents.

The voltammograms of dinuclear [Ru(tpy)(bpy)<sub>2</sub>(μ-R<sub>2</sub>R<sub>2'</sub>adpc)][PF<sub>6</sub>]<sub>2</sub> complexes present two quasi-reversible oxidation waves in the region between 0.6 and 1.7 V vs NHE. The first redox couple E<sub>1</sub> is further stabilized by about 400 mV from electron-releasing Me<sub>4</sub> to electron-withdrawing Cl<sub>4</sub> substituents, while the second redox couple E<sub>2</sub> does not vary much in its position. The assignment of these oxidation waves will be discussed on the basis of the results obtained from EPR and IR and UV–vis–NIR spectroelectrochemical studies.

**EPR Spectroscopy.** The EPR spectroscopic studies were performed on the singly oxidized dinuclear [ $\{\text{Ru}(\text{tpy})(\text{bpy})\}_2(\mu\text{-L})\]^{3+}$  complexes, where L = Me<sub>4</sub>adpc<sup>2-</sup> and Cl<sub>2</sub>adpc<sup>2-</sup> in an acetonitrile solution, and their spectra are shown in Figure 2. Unfortunately, acetonitrile solutions of [ $\{\text{Ru}(\text{tpy})(\text{bpy})\}_2(\mu\text{-L})\]^{3+}$ , where L = Me<sub>2</sub>adpc<sup>2-</sup>, adpc<sup>2-</sup>, and Cl<sub>4</sub>adpc<sup>2-</sup>, remained EPR-silent even at liquid-helium temperatures. [ $\{\text{Ru}(\text{tpy})(\text{bpy})\}_2(\mu\text{-Me}_4\text{adpc})\]^{3+}$  gave a room temperature isotropic spectrum in acetonitrile (Figure 2A) that is relatively narrow with g = 1.96. This is very similar to the EPR spectrum of the potassium salt of the 1,4-dicyanamide radical anion<sup>12</sup> for which g = 2.0023 and strongly suggests a SOMO

**Table 1. Quantitative Electronic Absorption Data<sup>a</sup> for  $Tl_2[R_2R'_2adpc]$  and  $[Ru(tpy)(bpy)]_2(\mu-R_2R'_2adpc)[PF_6]_2$  Complexes in DMF and Their Spectroelectrochemical Oxidation Products**

compound	absorption
$Me_2adpc^{2-}$	338 (4345), 515 (43600), 545 (37400)
$Me_2adpc^{\bullet-}$	430 (12000), 514 (33900), 667 (2440), 726 (9100), 1118 (760), 1256 (1780)
$adpc^{2-}$	340 (6700), 500 (54400), 523 (51500)
$adpc^{\bullet-}$	421 (8400), 498 (31100), 658 (5030), 714 (17400), 1310 (3900)
$Cl_2adpc^{2-}$	346 (6600), 506 (51000), 533 (50600)
$Cl_2adpc^{\bullet-}$	426 (15000), 505 (37600), 663 (2910), 719 (9130), 1175 (928), 1341 (2060)
$[Ru(tpy)(bpy)]_2(\mu-Me_4adpc)]^{2+}$	319 (58500), 501(62300)
$[Ru(tpy)(bpy)]_2(\mu-Me_4adpc)]^{3+}$	486 (42500), 652 (11300), 820 (10500), 1678 (5300)
$[Ru(tpy)(bpy)]_2(\mu-Me_4adpc)]^{4+}$	453 (42000), 696 (14500)
$[Ru(tpy)(bpy)]_2(\mu-Me_2adpc)]^{2+}$	321 (62000), 499 (69100)
$[Ru(tpy)(bpy)]_2(\mu-Me_2adpc)]^{3+}$	479 (44500), 652 (12800), 823 (12200), 1758 (7000)
$[Ru(tpy)(bpy)]_2(\mu-Me_2adpc)]^{4+}$	452 (44700), 652 (8400), 823 (7700)
$[Ru(tpy)(bpy)]_2(\mu-adpc)]^{2+}$	293 (81900), 317 (72100), 490 (69100)
$[Ru(tpy)(bpy)]_2(\mu-adpc)]^{3+}$	292 (86900), 314 (73700), 471 (41300), 652 (13900), 812 (12700), 1920 (10000)
$[Ru(tpy)(bpy)]_2(\mu-adpc)]^{4+}$	312 (73400), 456 (41900), 856 (12200)
$[Ru(tpy)(bpy)]_2(\mu-Cl_2adpc)]^{2+}$	321 (62000), 499 (69100)
$[Ru(tpy)(bpy)]_2(\mu-Cl_2adpc)]^{3+}$	482 (42300), 667 (13100), 833 (8700), 1923 (10400)
$[Ru(tpy)(bpy)]_2(\mu-Cl_2adpc)]^{4+}$	487 (25000), 668 (5300), 834 (6400), 1124 (11500)
$[Ru(tpy)(bpy)]_2(\mu-Cl_4adpc)]^{2+}$	321 (63700), 534 (60000)
$[Ru(tpy)(bpy)]_2(\mu-Cl_4adpc)]^{3+}$	517 (35900), 677 (7900), 876 (7700), 1923 (6600)
$[Ru(tpy)(bpy)]_2(\mu-Cl_4adpc)]^{4+}$	462 (31700), 677 (5660), 876 (7000), 1120 (7020)

<sup>a</sup>In DMF, 0.1 M TBAH,  $\lambda$  in nm,  $\epsilon$  in  $L mol^{-1} cm^{-1}$  in parentheses.

that is mostly localized on the bridging ligand and corresponds to the oxidation-state description  $[Ru^{II}, Me_4adpc^{\bullet-}, Ru^{II}]$ . On the other hand,  $[Ru(tpy)(bpy)]_2(\mu-Cl_2adpc)]^{3+}$  remained EPR-silent at room temperature and gave a broad anisotropic EPR signal at 110 K (Figure 2B) with  $g_1, g_2$ , and  $g_3 = 2.16, 2.09$ , and 1.96, respectively,  $g_{av} = 2.075$ , and  $g$  anisotropy  $\Delta g = g_1 - g_3 = 0.20$ . The spectral pattern is very similar to that of mononuclear  $[Ru(tpy)(bpy)(2,4-Cl_2pcyd)]^{2+}$ , for which  $g_1, g_2$ , and  $g_3 = 2.34, 2.10$ , and 1.92, respectively,<sup>13</sup> and is typical of a low-spin  $Ru^{III} d^5$  ion,<sup>13,14</sup> and this suggests the oxidation-state description of  $[Ru^{II}, Cl_2adpc^{2-}, Ru^{III}]^{3+}$  for  $[Ru(tpy)(bpy)]_2(\mu-Cl_2adpc)]^{3+}$ . However, this formal description should be qualified based on DFT calculations of  $[Ru(acac)_2(L)]^n$ , where  $n = 1-, 0$ , and  $1+$ , acac is acetylacetonate, and L is a redox-active ligand, which suggested that, for a similar range of  $g$  values, a pure  $Ru^{III}$  oxidation-state description is inaccurate and that significant spin density is located on the redox-active ligand.<sup>15</sup>

The EPR spectroscopy of the  $[Ru(tpy)(bpy)]_2(\mu-R_2R'_2adpc)]^{3+}$  complexes suggests that a transition has occurred from mostly ligand-centered to metal-centered spin

**Table 2. CV Data<sup>a</sup> for  $Tl_2[R_2R'_2adpc]$  and  $Ru(tpy)(bpy)$  Complexes**

ligand/complex	$E_1$	$E_2$	$\Delta E = E_2 - E_1$
$Tl_2[Me_2adpc]$	0.29 (60) <sup>b</sup>	0.43 (70) <sup>b</sup>	0.14
$Tl_2[adpc]$	0.40 (60) <sup>b</sup>	0.54 (67) <sup>b</sup>	0.14
$Tl_2[Cl_2adpc]$	0.47 (67) <sup>b</sup>	0.62 (67) <sup>b</sup>	0.15
$[Ru(tpy)(bpy)(2,4-Cl_2pcyd)] [PF_6]$	1.04 <sup>c</sup>		
$[Ru(tpy)(bpy)]_2(\mu-Me_4adpc) [PF_6]_2$	0.67 (59) <sup>d</sup>	1.59 (74) <sup>d</sup>	0.92
$[Ru(tpy)(bpy)]_2(\mu-Me_2adpc) [PF_6]_2$	0.70 (64) <sup>d</sup>	1.56 (82) <sup>d</sup>	0.86
$[Ru(tpy)(bpy)]_2(\mu-adpc) [PF_6]_2$	0.80 (59) <sup>d</sup>	1.56 (71) <sup>d</sup>	0.76
$[Ru(tpy)(bpy)]_2(\mu-Cl_2adpc) [PF_6]_2$	0.94 (66) <sup>d</sup>	1.60 (80) <sup>d</sup>	0.66
$[Ru(tpy)(bpy)]_2(\mu-Cl_4adpc) [PF_6]_2$	1.06 (114) <sup>d</sup>	1.61 (74) <sup>d</sup>	0.55

<sup>a</sup>In V vs NHE (anodic and cathodic peak separation in mV), scan rate 0.1 V/s, in 0.1 M tetrabutylammonium hexafluorophosphate,  $Fc^+/Fc$  used as the internal reference. <sup>b</sup>In DMF. <sup>c</sup>Taken from ref 11. <sup>d</sup>In acetonitrile.

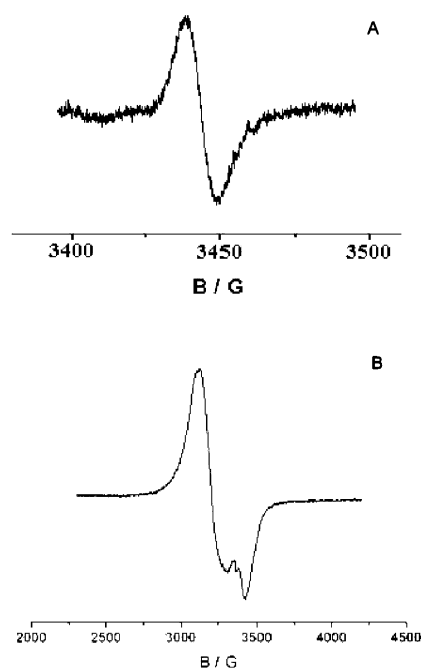
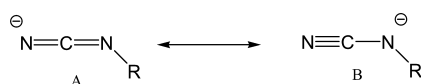


**Figure 2.** EPR spectra of  $[Ru(tpy)(bpy)]_2(\mu-L)]^{3+}$  in acetonitrile: (A)  $L = Me_4adpc^{2-}$  at 295 K; (B)  $L = Cl_2adpc^{2-}$  at 10 K.

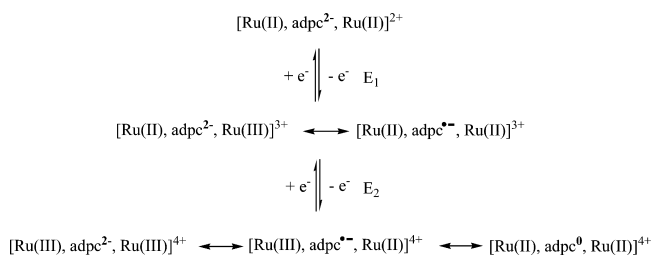
density with a change in the R and R' substituents from electron-donating to electron-withdrawing properties. The greater stability of  $Cl_2adpc^{2-}$  to oxidation (Table 2) compared to  $Me_4adpc^{2-}$  is the probable reason for this transition. The consistency of this interpretation will be examined by the complexes' IR and vis-NIR spectroelectrochemistry.

**IR Spectroelectrochemistry.** For ruthenium cyanamide complexes, the  $\nu(NCN)$  band frequency is dependent on the ruthenium oxidation state. The reason for this is that the cyanamide anion possesses two resonance forms



which contribute to bonding in the cyanamide group and the frequency of  $\nu(\text{NCN})$ . The population of resonance forms can be perturbed by coordination to a metal ion and the nature of the coordination sphere. When the cyanamide group is bonded to the  $\pi$ -acid  $\text{Ru}^{\text{III}}$  ion, the contribution of resonance form **A** increases and  $\nu(\text{NCN})$  approaches that of an organic carbodiimide (range of  $2100\text{--}2150\text{ cm}^{-1}$ ).<sup>16</sup> If the cyanamide group is bonded to the  $\pi$ -donor  $\text{Ru}^{\text{II}}$  ion, resonance form **B** increases its contribution and  $\nu(\text{NCN})$  approaches that of a neutral cyanamide (ca.  $2250\text{ cm}^{-1}$ ).<sup>17</sup> Thus, for a given  $\text{Ru}^{\text{II}}$  coordination sphere, oxidation to  $\text{Ru}^{\text{III}}$  results in a shift of  $\nu(\text{NCN})$  to lower frequencies. This has been shown in IR spectroelectrochemical studies of  $[\text{Ru}(\text{tpy})(\text{bpy})(2,4\text{-Cl}_2\text{pcyd})]^+$ ,  $[\text{Ru}(\text{NH}_3)_5(2,3,5,6\text{-Cl}_4\text{pcyd})]^+$ , and  $[\text{Ru}(\text{NH}_3)_3(\text{bpy})(2,3\text{-Cl}_2\text{pcyd})]^+$  complexes.<sup>13,18</sup> Because the IR time scale is on the order of  $10^{13}\text{ s}^{-1}$ , the number of  $\nu(\text{NCN})$  bands observed is a good measure of whether a mixed-valence complex is valence-trapped or delocalized.<sup>19</sup> For symmetric mixed-valence complexes incorporating a bridging  $\text{adpc}^{2-}$  ligand, two cyanamide  $\nu(\text{NCN})$  bands are predicted if valence-trapped, whereas only one is predicted if delocalized. If instead the bridging  $\text{adpc}^{2-}$  ligand is oxidized to a radical anion, delocalization within the radical is expected to result in the observation of only one  $\nu(\text{NCN})$  band. The one-electron oxidation of  $[\text{Ru}(\text{tpy})(\text{bpy})_2(\mu\text{-adpc})]^{2+}$  to  $[\text{Ru}(\text{tpy})(\text{bpy})_2(\mu\text{-adpc})]^{3+}$  and two-electron oxidation to  $[\text{Ru}(\text{tpy})(\text{bpy})_2(\mu\text{-adpc})]^{4+}$  are summarized in terms of possible oxidation-state descriptions in Scheme 4.

#### Scheme 4. Oxidation-State Descriptions for One- and Two-Electron Oxidation of $[\{\text{Ru}(\text{tpy})(\text{bpy})_2(\mu\text{-adpc})\}^{2+}]^{2+}$



IR spectroelectrochemistry in the region of  $\nu(\text{NCN})$  for the  $[\{\text{Ru}(\text{tpy})(\text{bpy})_2(\mu\text{-L})\}][\text{PF}_6]_2$  complexes, where  $\text{L} = \text{Me}_4\text{adpc}^{2-}$ ,  $\text{adpc}^{2-}$ , and  $\text{Cl}_2\text{adpc}^{2-}$ , in DMF is shown in Figures 3–5. Those for  $\text{L} = \text{Me}_2\text{adpc}^{2-}$  and  $\text{Cl}_4\text{adpc}^{2-}$  are very similar to those for  $\text{L} = \text{Me}_4\text{adpc}^{2-}$  and  $\text{Cl}_2\text{adpc}^{2-}$ , respectively, and have been placed in the SI (Figures S15 and S16). All complexes show good reversibility (>95%) upon single-electron oxidation to  $[\{\text{Ru}(\text{tpy})(\text{bpy})_2(\mu\text{-L})\}]^{3+}$ , while the second oxidation is not very reversible (less than 90% recovery of the initial spectrum).

Figure 3 shows the IR spectra resulting from the one- and two-electron oxidations of  $[\{\text{Ru}(\text{tpy})(\text{bpy})_2(\mu\text{-Me}_4\text{adpc})\}^{2+}]^{2+}$ . In Figure 3A, oxidation to the trication is accompanied by a large decrease in the intensity of the  $\nu(\text{NCN})$  band at  $2160\text{ cm}^{-1}$  together with a slight shift to higher frequencies. On the basis of EPR studies (Figure 2A), this change is associated with the formation of radical anion  $\text{Me}_4\text{adpc}$  and the oxidation-state description  $[\text{Ru}^{\text{II}}, \text{Me}_4\text{adpc}^{\bullet-}, \text{Ru}^{\text{II}}]^{3+}$  in Scheme 4. Further oxidation (Figure 3B) shows the growth of a weak band at  $2030\text{ cm}^{-1}$ , which is consistent with anionic cyanamide bound to  $\text{Ru}^{\text{III}}$  and suggests an oxidation-state description  $[\text{Ru}^{\text{II}}$ ,

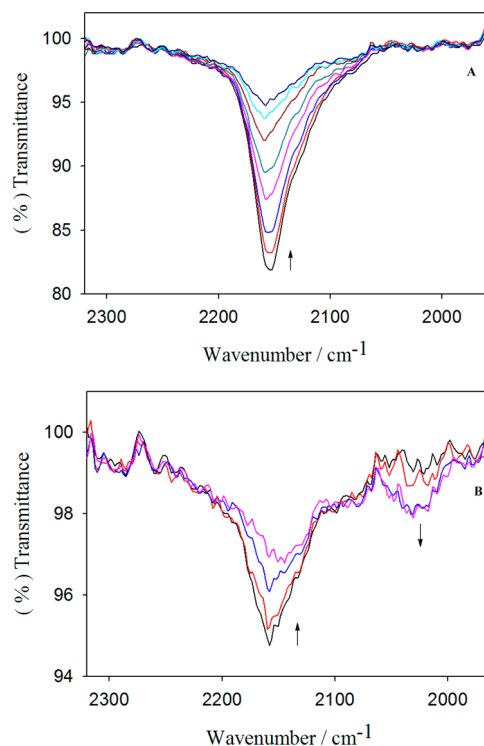


**Figure 3.** IR spectroelectrochemical oxidation of (A)  $[\{\text{Ru}(\text{tpy})(\text{bpy})_2(\mu\text{-Me}_4\text{adpc})\}^{2+}]^{2+}$  forming  $[\{\text{Ru}(\text{tpy})(\text{bpy})_2(\mu\text{-Me}_4\text{adpc})\}^{3+}]^{3+}$  and (B) the trication complex forming  $[\{\text{Ru}(\text{tpy})(\text{bpy})_2(\mu\text{-Me}_4\text{adpc})\}^{4+}]^{4+}$  in DMF, 0.1 M TBAH: (A) 0–0.58 V and (B) 0.58–0.70 V vs Ag/AgCl.

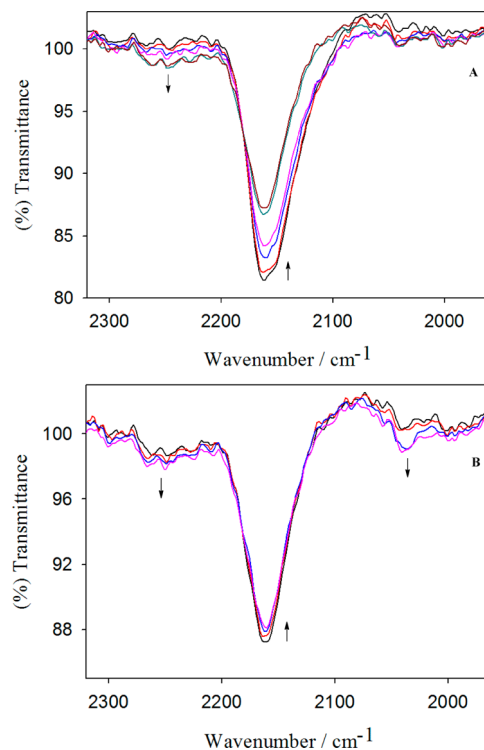


**Figure 4.** IR spectroelectrochemical oxidation of (A)  $[\{\text{Ru}(\text{tpy})(\text{bpy})_2(\mu\text{-adpc})\}^{2+}]^{2+}$  forming  $[\{\text{Ru}(\text{tpy})(\text{bpy})_2(\mu\text{-adpc})\}^{3+}]^{3+}$  and (B) the trication complex forming  $[\{\text{Ru}(\text{tpy})(\text{bpy})_2(\mu\text{-adpc})\}^{4+}]^{4+}$  in DMF, 0.1 M TBAH: (A) 0–0.66 V and (B) 0.66–0.80 V vs Ag/AgCl.

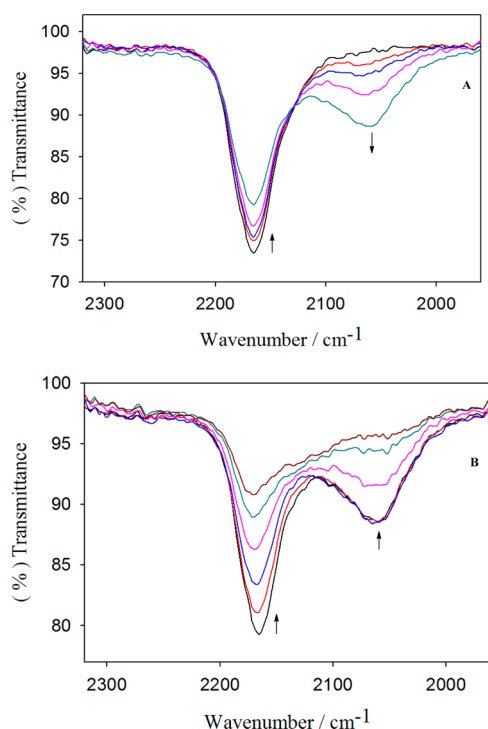


**Figure 5.** IR spectroelectrochemical oxidation of (A)  $[\{\text{Ru}(\text{tpy})(\text{bpy})\}_2(\mu\text{-Cl}_2\text{adpc})]^{2+}$  forming  $[\{\text{Ru}(\text{tpy})(\text{bpy})\}_2(\mu\text{-Cl}_2\text{adpc})]^{3+}$  and (B) the trication complex forming  $[\{\text{Ru}(\text{tpy})(\text{bpy})\}_2(\mu\text{-Cl}_2\text{adpc})]^{4+}$  in DMF, 0.1 M TBAH: (A) 0–0.66 V and (B) 0.66–0.82 V vs Ag/AgCl.

$\text{Me}_4\text{adpc}^{\bullet-}$ ,  $\text{Ru}^{\text{III}}]^{4+}$ . For  $[\{\text{Ru}(\text{tpy})(\text{bpy})\}_2(\mu\text{-adpc})]^{2+}$ , oxidation gives significantly different spectral changes in the region of  $\nu(\text{NCN})$  (see Figure 4).

The main feature of both parts A and B of Figure 4 is a single  $\nu(\text{NCN})$  band, and this is consistent with a symmetric state in which the oxidation-state descriptions are delocalized  $[\text{Ru}^{\text{II}}, \text{adpc}^{2-}, \text{Ru}^{\text{III}}]^{3+}$  and  $[\text{Ru}^{\text{III}}, \text{adpc}^{2-}, \text{Ru}^{\text{III}}]^{4+}$ , respectively. However, there are additional weak bands that are difficult to rationalize. In Figure 4A, oxidation to the mixed-valence complex  $[\{\text{Ru}(\text{tpy})(\text{bpy})\}_2(\mu\text{-adpc})]^{3+}$  results in a moderate decrease in the intensity of the band at  $2160\text{ cm}^{-1}$  that is accompanied by the growth of a weak band at  $2265\text{ cm}^{-1}$ . The band at  $2265\text{ cm}^{-1}$  is similar to that seen for protonated cyanamides ( $\text{adpcH}_2$  has  $\nu(\text{NCN}) = 2225\text{ cm}^{-1}$ ) and may be due to a neutral radical cyanamide group  $\nu(\text{NCN})$ . However, this would require valence trapping of  $\text{adpc}^{\bullet-}$ , with a neutral radical cyanamide at one end and an anionic cyanamide at the other. This is unlikely because there is no barrier for delocalization and indeed only one  $\nu(\text{NCN})$  band is observed for a complex with  $\text{Me}_4\text{adpc}^{\bullet-}$  (Figure 3A). Further oxidation (Figure 4B) only slightly decreases the band at  $2160\text{ cm}^{-1}$  and slightly increases the weak band at  $2250\text{ cm}^{-1}$  but sees the growth of a weak intensity band at  $2030\text{ cm}^{-1}$  that may be a  $\nu(\text{NCN})$  due to an anionic cyanamide bound to  $\text{Ru}^{\text{III}}$ . Thus, there appear to be  $\nu(\text{NCN})$  bands that are consistent with all three oxidation-state descriptions of the tetracation in Scheme 4. The oxidation of  $[\{\text{Ru}(\text{tpy})(\text{bpy})\}_2(\mu\text{-Cl}_2\text{adpc})]^{2+}$  shows significantly less complexity (Figure 5).

In Figure 5A, oxidation forming the mixed-valence complex  $[\{\text{Ru}(\text{tpy})(\text{bpy})\}_2(\mu\text{-Cl}_2\text{adpc})]^{3+}$  results in a decrease of the  $\nu(\text{NCN})$  band at  $2160\text{ cm}^{-1}$  and the growth of a band at  $2040\text{ cm}^{-1}$ . The observation of two  $\nu(\text{NCN})$  bands and an EPR spectrum of a low-symmetry  $\text{Ru}^{\text{III}}$  ion (Figure 2b) is entirely

consistent with a valence-trapped oxidation-state description  $[\text{Ru}^{\text{II}}, \text{Cl}_2\text{adpc}^{2-}, \text{Ru}^{\text{III}}]^{3+}$ . Further oxidation forming  $[\{\text{Ru}(\text{tpy})(\text{bpy})\}_2(\mu\text{-Cl}_2\text{adpc})]^{4+}$  shows a loss of the low-frequency band and a further decrease in the  $\nu(\text{NCN})$  band at  $2160\text{ cm}^{-1}$ . A single band is consistent with the oxidation-state description  $[\text{Ru}^{\text{III}}, \text{Cl}_2\text{adpc}^{2-}, \text{Ru}^{\text{III}}]^{4+}$  or  $[\text{Ru}^{\text{II}}, \text{Cl}_2\text{adpc}^0, \text{Ru}^{\text{II}}]^{4+}$  in Scheme 4, but the latter state description seems unlikely because  $\nu(\text{NCN})$  for this description should have a much greater frequency.

As shown by Figures 3–5, significant differences in the observed  $\nu(\text{NCN})$  bands occur depending on the appropriate oxidation-state description in Scheme 4. It remains to explore how these oxidation-state descriptions influence the electronic absorption spectroscopy of these systems.

**Vis–NIR Spectroelectrochemistry.** The vis–NIR spectroelectrochemical oxidation of  $\text{Cl}_2\text{adpc}^{2-}$  in DMF is representative of the  $\text{R}_2\text{R}'_2\text{adpc}^{2-}$  ions. As shown in Figure 6,

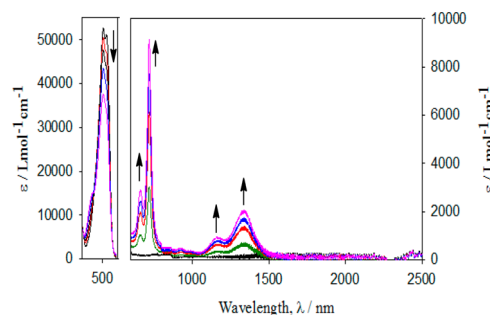


**Figure 6.** Vis–NIR spectroelectrochemical oxidation of  $\text{Cl}_2\text{adpc}^{2-}$  forming radical anion  $\text{Cl}_2\text{adpc}^{\bullet-}$  in DMF, 0.1 M TBAH: 0–0.80 V vs Ag/AgCl.

oxidation to the radical anion  $\text{Cl}_2\text{adpc}^{\bullet-}$  results in a moderate decrease in the ICT band<sup>1</sup> at 500 nm and the growth of two bands at 715 and 1315 nm of weaker intensity. Further oxidation of the radical to  $\text{Cl}_2\text{adpc}^0$  proved to be irreversible.

The vis–NIR spectroelectrochemical oxidation of  $[\{\text{Ru}(\text{tpy})(\text{bpy})\}_2(\mu\text{-L})]^{2+}$  complexes, where  $\text{L} = \text{Me}_4\text{adpc}^{2-}$ ,  $\text{adpc}^{2-}$ , and  $\text{Cl}_2\text{adpc}^{2-}$ , in DMF is shown in Figures 7–9, and spectral data are found in Table 1. Those for  $\text{L} = \text{Me}_2\text{adpc}^{2-}$  and  $\text{Cl}_4\text{adpc}^{2-}$  have been placed in the SI (Figures S17 and S18). For one-electron oxidation, the spectroscopic changes seen in Figures 7A–9A are similar but show significant differences that must be related to the noninnocence of the  $\text{R}_2\text{R}'_2\text{adpc}^{2-}$  ligand and the change in the oxidation-state description of the complexes. In Figure 7A, oxidation of  $[\{\text{Ru}(\text{tpy})(\text{bpy})\}_2(\mu\text{-Me}_4\text{adpc})]^{2+}$  to the trication results in a decrease in the ICT band at 501 nm and the growth of bands at 652, 820, and 1678 nm. On the basis of the trication's EPR spectrum (Figure 2A), the assigned oxidation-state description  $[\text{Ru}^{\text{II}}, (\text{Me}_4\text{adpc}^{\bullet-}, \text{Ru}^{\text{II}})]^{3+}$ , and the spectrum of  $\text{Cl}_2\text{adpc}^{\bullet-}$  (Figure 6), it seems reasonable to assign the bands at 652, 820, and 1678 nm to ICT transitions of  $\text{Me}_4\text{adpc}^{\bullet-}$  with possibly some MLCT character mixed into the low-energy bands. For  $[\{\text{Ru}(\text{tpy})(\text{bpy})\}_2(\mu\text{-adpc})]^{3+}$  (Figure 8A), a broad absorption appears at ca. 1000 nm, which for  $[\{\text{Ru}(\text{tpy})(\text{bpy})\}_2(\mu\text{-Cl}_2\text{adpc})]^{3+}$  (Figure 9A) resolves itself to a band at 1124 nm. Upon two-electron oxidation to  $[\{\text{Ru}(\text{tpy})(\text{bpy})\}_2(\mu\text{-Cl}_2\text{adpc})]^{4+}$  (Figure 9B), this band becomes a dominant feature with  $\lambda_{\text{max}} = 1124\text{ nm}$ , and on the basis of the oxidation-state description  $[\text{Ru}^{\text{III}}, \text{Cl}_2\text{adpc}^{2-}, \text{Ru}^{\text{III}}]^{4+}$ , we assign this band to a cyanamide-to- $\text{Ru}^{\text{III}}$  LMCT transition.<sup>11</sup>

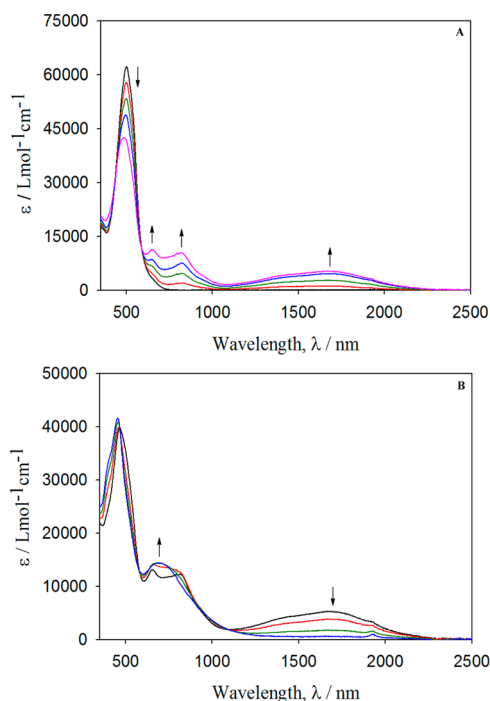


**Figure 7.** Vis–NIR spectroelectrochemical oxidation of  $[\{\text{Ru}(\text{tpy})(\text{bpy})\}_2(\mu\text{-Me}_4\text{adpc})]^{2+}$  forming (A)  $[\{\text{Ru}(\text{tpy})(\text{bpy})\}_2(\mu\text{-Me}_4\text{adpc})]^{3+}$  and (B)  $[\{\text{Ru}(\text{tpy})(\text{bpy})\}_2(\mu\text{-Me}_4\text{adpc})]^{4+}$  in DMF, 0.1 M TBAH: (A) 0–0.48 V and (B) 0.50–0.58 V vs Ag/AgCl.

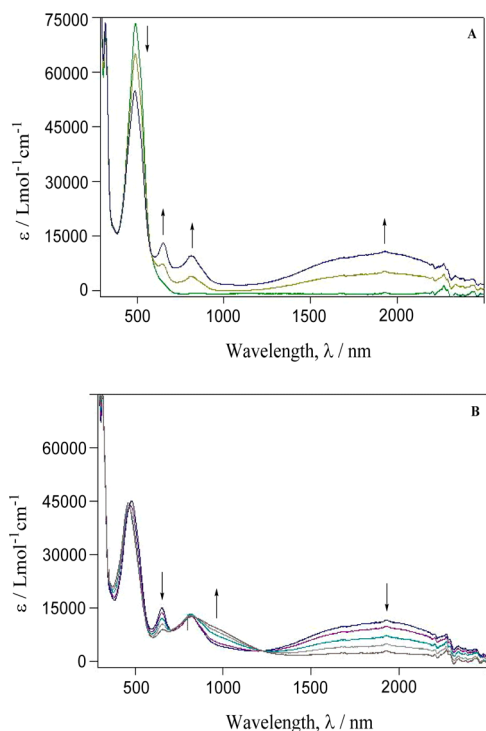


**Figure 8.** Vis–NIR spectroelectrochemical oxidation of  $[\{\text{Ru}(\text{tpy})(\text{bpy})\}_2(\mu\text{-adpc})]^{2+}$  forming (A)  $[\{\text{Ru}(\text{tpy})(\text{bpy})\}_2(\mu\text{-adpc})]^{3+}$  and (B)  $[\{\text{Ru}(\text{tpy})(\text{bpy})\}_2(\mu\text{-adpc})]^{4+}$  in DMF, 0.1 M TBAH: (A) 0–0.75 V and (B) 0.80–1.00 V vs Ag/AgCl.

Another important change that occurs in Figures 7–9 is that the low-energy NIR band red shifts and becomes noticeably broader with the donor/withdrawing properties of the

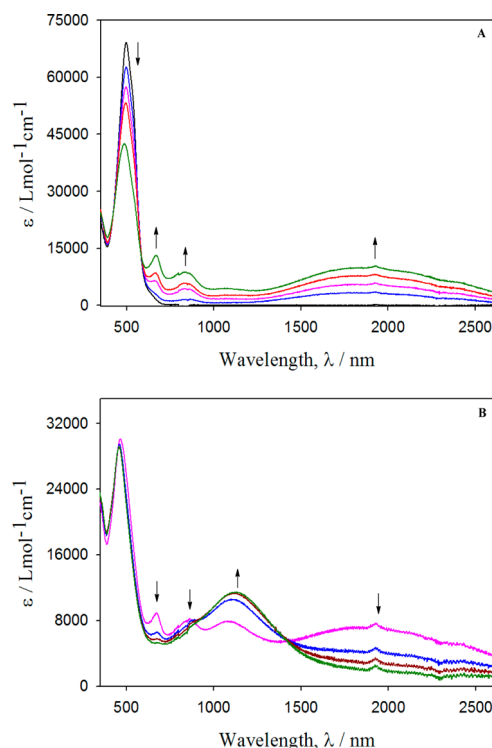


**Figure 9.** Vis–NIR spectroelectrochemical oxidation of (A)  $[\{\text{Ru}(\text{tpy})(\text{bpy})\}_2(\mu\text{-Cl}_2\text{adpc})]^{2+}$  forming  $[\{\text{Ru}(\text{tpy})(\text{bpy})\}_2(\mu\text{-Cl}_2\text{adpc})]^{3+}$  and (B) forming  $[\{\text{Ru}(\text{tpy})(\text{bpy})\}_2(\mu\text{-Cl}_2\text{adpc})]^{4+}$  in DMF, 0.1 M TBAH: (A) 0–0.78 V and (B) 0.81–0.98 V vs Ag/AgCl.

$\text{R}_2\text{R}'_2\text{adpc}$  substituent. These changes to the NIR band for the trication complexes are summarized in Table 3.

**Table 3.** NIR Band Properties of  $[\{\text{Ru}(\text{tpy})(\text{bpy})\}_2(\mu\text{-L})]^{3+}$  Complexes

L	$E_{\text{op}}, \text{cm}^{-1}$	intensity $\epsilon, \text{L mol}^{-1} \text{cm}^{-1}$	oscillator strength $f^a$
$\text{Me}_4\text{adpc}^{2-}$	5960	5300	0.074
$\text{Me}_2\text{adpc}^{2-}$	5668	7000	0.098
$\text{adpc}^{2-}$	5208	11000	0.141
$\text{Cl}_2\text{adpc}^{2-}$	5200	10400	0.167
$\text{Cl}_4\text{adpc}^{2-}$	5200	6600	0.118

<sup>a</sup>The oscillator strength was calculated by summing the oscillator strengths of Gaussian peaks used to model the NIR band envelope.

As supported by EPR and IR spectroelectrochemical studies, the  $[\{\text{Ru}(\text{tpy})(\text{bpy})\}_2(\mu\text{-L})]^{3+}$  complexes, where  $\text{L} = \text{adpc}^{2-}$ ,  $\text{Cl}_2\text{adpc}^{2-}$ , and  $\text{Cl}_4\text{adpc}^{2-}$ , possess an oxidation-state description  $[\text{Ru}^{\text{II}}, \text{R}_2\text{R}'_2\text{adpc}^{2-}, \text{Ru}^{\text{III}}]^{3+}$ , and it is then appropriate to describe their NIR band as an intervalence transition. Although the data are limited in Table 3, it is suggested that the shift in  $E_{\text{op}}$  to higher energies with substituent donor properties is an indicator of increasing radical anion  $\text{R}_2\text{R}'_2\text{adpc}$  character. We attempted to model this change using theory, but DFT calculations including solvent perturbations would not converge.

## CONCLUSION

The synthetic chemistry of substituted azobis(phenylcyanamide) ligands is presented. Electron-withdrawing substituents deactivate azodianilines and limit the synthetic pathways to cyanamides. The complexes  $[\{\text{Ru}(\text{tpy})(\text{bpy})\}_2(\mu\text{-$

L)] $[\text{PF}_6]_2$ , where L =  $\text{Me}_4\text{adpc}^{2-}$ ,  $\text{Me}_2\text{adpc}^{2-}$ ,  $\text{adpc}^{2-}$ ,  $\text{Cl}_2\text{adpc}^{2-}$ , and  $\text{Cl}_4\text{adpc}^{2-}$ , were prepared and characterized by CV and vis–NIR and IR spectroelectrochemistry. The EPR spectrum of  $[\{\text{Ru}(\text{tpy})(\text{bpy})\}_2(\mu\text{-Me}_4\text{adpc})]^{3+}$  showed an organic radical signal and is consistent with an oxidation-state description  $[\text{Ru}^{\text{II}}, \text{Me}_4\text{adpc}^{\bullet-}, \text{Ru}^{\text{II}}]^{3+}$ , while that of  $[\{\text{Ru}(\text{tpy})(\text{bpy})\}_2(\mu\text{-Cl}_2\text{adpc})]^{3+}$  showed a low-symmetry  $\text{Ru}^{\text{III}}$  signal, which is consistent with the description  $[\text{Ru}^{\text{III}}, \text{Cl}_2\text{adpc}^{2-}, \text{Ru}^{\text{II}}]^{3+}$ . IR spectroelectrochemistry of the  $[\{\text{Ru}(\text{tpy})(\text{bpy})\}_2(\mu\text{-L})]^{3+}$  complexes suggested that, for L =  $\text{Me}_4\text{adpc}^{2-}$  and  $\text{Me}_2\text{adpc}^{2-}$  complexes, the bridging ligand is a radical anion, while for L =  $\text{adpc}^{2-}$ ,  $\text{Cl}_2\text{adpc}^{2-}$ , and  $\text{Cl}_4\text{adpc}^{2-}$ , the oxidation-state description  $[\text{Ru}^{\text{III}}, \text{L}^{2-}, \text{Ru}^{\text{II}}]^{3+}$  is appropriate. Furthermore, IR data suggest that  $[\{\text{Ru}(\text{tpy})(\text{bpy})\}_2(\mu\text{-adpc})]^{3+}$  is delocalized and  $[\{\text{Ru}(\text{tpy})(\text{bpy})\}_2(\mu\text{-Cl}_2\text{adpc})]^{3+}$  and  $[\{\text{Ru}(\text{tpy})(\text{bpy})\}_2(\mu\text{-Cl}_4\text{adpc})]^{3+}$  are valence-trapped mixed-valence systems. The transition between oxidation-state descriptions of the complexes  $[\{\text{Ru}(\text{tpy})(\text{bpy})\}_2(\mu\text{-L})]^{3+}$  is also examined by its effect on the complexes' electronic spectra. For  $[\{\text{Ru}(\text{tpy})(\text{bpy})\}_2(\mu\text{-L})]^{3+}$ , the NIR band is unique to the trication, but its energy and intensity vary depending on its oxidation-state description.

In summary, the tricationic dinuclear ruthenium complexes are shown by EPR and IR and vis–NIR spectroelectrochemistry to have properties that switch between oxidation-state descriptions  $[\text{Ru}^{\text{II}}, \text{adpc}^{\bullet-}, \text{Ru}^{\text{II}}]^{3+}$  and  $[\text{Ru}^{\text{III}}, \text{adpc}^{2-}, \text{Ru}^{\text{II}}]^{3+}$  depending on the donor–acceptor properties of the substituents on  $\text{adpc}^{2-}$ . This study reveals in a single system a transformation from bridging ligand noninnocence to mixed-valent class III and II properties.

## EXPERIMENTAL SECTION

**Materials.** All of the reagents and solvents were reagent-grade or better and were purchased from Aldrich, Acros, and Strem Chemicals. The syntheses of reagent azodianilines and complexes are described in the SI. Indium–tin oxide (ITO) glass plates were purchased from Delta Technologies, and gold foil was purchased from Buckbee Mears.  $\text{Ti}_2[\text{adpc}]$  and  $[\{\text{Ru}(\text{tpy})(\text{bpy})\}_2(\mu\text{-adpc})][\text{PF}_6]_2$  have been previously reported.<sup>1</sup> The reagent complexes  $\text{Ru}(\text{tpy})\text{Cl}_3\cdot\text{H}_2\text{O}$  and  $[\text{Ru}(\text{tpy})(\text{bpy})\text{Cl}][\text{PF}_6]_2$  were prepared following modified literature procedures (see the SI).<sup>20,21</sup>

**Instrumentation.** BOMEM Michelson MB100 Fourier transform infrared and Cary 5 UV–vis–NIR spectrophotometers were used to record IR and electronic spectra, respectively. <sup>1</sup>H NMR spectra were obtained at ambient temperature using a Bruker AMX-400 NMR or a Bruker 300 Ultra Shield spectrometer and referenced to tetramethylsilane (0.00 ppm). CV studies were performed with a Metrohm Autolab PGSTAT30 potentiostat/galvanostat on argon-saturated solutions of the complexes in DMF with 0.1 M TBAH as the supporting electrolyte. A three-electrode arrangement consisting of a platinum disk working electrode (BAS; 1.6 mm diameter), a platinum wire auxiliary electrode, and Ag/AgCl quasi-reference electrode was used. The electrochemical cell consisted of a double-jacketed glass container with an internal volume of 15 mL. Ferrocene ( $E^\circ = 0.665$  V vs NHE)<sup>22</sup> was used for calibration. UV–vis–NIR spectroelectrochemistry of all dinuclear complexes and anionic ligands was performed by using an optically transparent thin-layer electrochemistry (OTTLE) cell.<sup>18,23</sup> The cell had interior dimensions of roughly 1 × 2 cm with a path length of 0.2 cm and was fitted with a AgCl/Ag quasi-reference electrode. ITO-coated glass served as working and counter electrodes. UV–vis–NIR spectra were obtained on a Cary 5 spectrophotometer, and the potential was controlled by using a BAS CV-27 potentiostat. At any given potential, the system was allowed to come to equilibrium ( $i \approx 0$   $\mu\text{A}$ ) before the spectrum was taken. IR spectroelectrochemistry was performed using the OTTLE cell described above using a gold foil (500 line/in. and 60% transmittance)

as working and counter electrodes and Ag/AgCl as the quasi-reference electrode. EPR spectra of the complexes were recorded in acetonitrile at room temperature to 10 K by using a Bruker system EMX, and a ESR 900 continuous-flow cryostat from Oxford Instruments was used for this purpose. Jandel Peakfit was used to model the NIR charge-transfer bands.

**Syntheses of Azobis(phenylcyanamide) Ligands.** *3,3'-Dichloro-4,4'-azobis(phenylcyanamide)·0.25H<sub>2</sub>O*,  $\text{Cl}_2\text{adpcH}_2$ . A boiling solution of benzoyl chloride (2 g, 14.2 mmol) in 20 mL of acetone was added dropwise to a refluxing solution of  $\text{NH}_4\text{SCN}$  (1.08 g, 14.2 mmol) in 20 mL of acetone for 30 min. To the mixture was added a boiling solution of 3,3'-dichloro-4,4'-azodianiline (1.25 g, 4.7 mmol) in acetone (100 mL) and the reflux continued for 12 h. The resulting suspension was added to 1 L of distilled water to afford precipitation of the orange benzoylthiourea derivative, which was then filtered, washed with water, and then added to a boiling solution of 2 M NaOH (400 mL) and stirred vigorously for about 20 min until a deep-red solution formed. The solution was cooled to 60–65 °C and treated with a solution of lead acetate (5.36 g, 14.2 mmol) in distilled water (20 mL) while stirring to effect precipitation of black PbS. After 5 min, the reaction mixture was filtered through a Buchner funnel into an ice-cooled suction flask. The dark-red filtrate was then acidified with glacial acetic acid (100 g, 1.67 mol), precipitating a dark-green product. Recrystallization from 1.6 L of boiling acetone afforded 1.05 g of a yellowish-green product. Yield: 71.3%. Anal. Calcd for  $\text{C}_{14}\text{H}_{8.5}\text{N}_6\text{O}_{0.25}\text{Cl}_2$ : C, 50.10; H, 2.55; N, 25.04. Found: C, 50.25; H, 2.64; N, 25.00. <sup>1</sup>H NMR (300 MHz,  $\text{DMSO}-d_6$ ): 10.51 (2H, s), 7.96 (2H, d), 7.93 (2H, dd), 7.39 (2H, d). IR (KBr):  $\nu(\text{NCN})$  2248  $\text{cm}^{-1}$ . Mass spectrum:  $m/z$  331 ( $\text{M}^+$ ).

*2,2':5,5'-Tetrachloro-4,4'-azobis(phenylcyanamide)*,  $\text{Cl}_4\text{adpcH}_2$ . The synthesis was similar to that above with some modification: 4 equiv of  $\text{NH}_4\text{SCN}$  and benzoyl chloride were used for the preparation of benzoyl thiocyanate, which was then refluxed with 1 equiv of 2,2':5,5'-tetrachloro-4,4'-azodianiline in almost double the volume of acetone for 36 h to generate the crude product. <sup>1</sup>H NMR showed the crude to be made of mostly  $\text{Cl}_2\text{adpcH}_2$  (~80%) and an impurity (likely monocyanamide). The poor solubility frustrated attempts at purification, and so the compound was used as isolated to make its thallium salt (see below). <sup>1</sup>H NMR (300 MHz,  $\text{DMSO}-d_6$ ): 7.71 (2H, s), 7.27 (2H, s). IR (KBr):  $\nu(\text{NCN})$  2251  $\text{cm}^{-1}$ .

*2,2':5,5'-Tetramethyl-4,4'-azobis(phenylcyanamide)·0.4acetone·0.2CH<sub>3</sub>COOH*,  $\text{Me}_4\text{adpcH}_2$ . The synthesis was similar to that of  $\text{Cl}_2\text{adpcH}_2$  except that crude  $\text{Me}_4\text{adpcH}_2$  was recrystallized from acetone/water/glacial acetic acid (1:1:1) to give yellow crystalline flakes in 50% final yield. Anal. Calcd for  $\text{C}_{19.6}\text{H}_{21.2}\text{N}_6\text{O}_{0.8}$ : C, 66.57; H, 6.04; N, 23.77. Found: C, 66.35; H, 5.69; N, 23.70. <sup>1</sup>H NMR (300 MHz,  $\text{DMSO}-d_6$ ): 9.67 (2H, s), 7.45 (2H, s), 7.04 (2H, s), 2.65 (6H, s), 2.21 (6H, s). IR (KBr):  $\nu(\text{NCN})$  2233  $\text{cm}^{-1}$ . Mass spectrum:  $m/z$  318 ( $\text{M}^+$ ). The presence of acetone and acetic acid was confirmed by <sup>1</sup>H NMR. Integration was consistent with the above formula.

*4,4'-Azobis(phenylcyanamide)*,  $\text{adpcH}_2$ .  $\text{adpcH}_2$  was prepared previously<sup>5</sup> using method 1 (Scheme 1) and gave a reported yield of 50%. Two alternative procedures are presented below.

Method 2 (Scheme 2). To 4,4'-azodianiline (1.0 g, 4.7 mmol) in 60 mL of 40% DMF in glacial acetic acid was added half of a solution of CNBr (1.20 g, 11.3 mmol) in 20 mL of 40% DMF in glacial acetic acid, and the resulting solution was stirred at –10 to –15 °C for 30 min. The rest of the CNBr solution was then added to the reaction mixture, followed by the dropwise addition of 20 mL of a 1 M NaOH solution over 1 h. The reaction mixture was permitted to rise to room temperature and stirred for 24 h, precipitating golden-yellow microcrystalline  $\text{adpcH}_2$ , which was filtered, washed with a copious amount of water, and dried overnight. Yield: 1.21 g, 95%. Anal. Calcd for  $\text{adpcH}_2\cdot\text{H}_2\text{O}$ ,  $\text{C}_{14}\text{H}_{12}\text{N}_6\text{O}$ : C, 59.99; H, 4.32; N, 29.98. Found: C, 59.70; H, 4.39; N, 29.76. <sup>1</sup>H NMR (300 MHz,  $\text{DMSO}-d_6$ ): 10.61 (2H, s), 7.88 (4H, d), 7.12 (4H, d). IR (KBr):  $\nu(\text{NCN})$  2225  $\text{cm}^{-1}$ , in agreement with the literature.<sup>1</sup>

Method 3 (Scheme 3). To a solution of 4,4'-azodianiline (1.0 g, 4.7 mmol) in tetrahydrofuran (THF; 100 mL) was added dropwise about 4.5 mL (10.62 mmol) of a 2.5 M BuLi solution in hexane at –30 to

−40 °C, and the mixture was stirred for 30 min, during which time the dark-brown solution turned red because of formation of the corresponding amide. The solution was then brought to room temperature, and CS<sub>2</sub> (0.7 mL, 11.2 mmol) was added. The resulting mixture was then stirred at room temperature for 24 h, during which time an orange precipitate was formed. The precipitate was filtered, washed with THF, and dried overnight to obtain 0.85 g of pure lithium dithiocarbamate (yield: 48%). To a solution of dithiocarbamate (0.3 g, 0.80 mmol) in acetonitrile (50 mL) was added concentrated NH<sub>3</sub> (30 mL), and the temperature of the solution was brought down to 0 to −5 °C. Diacetoxyiodobenzene (DIB; 0.26 g, 0.80 mmol) was added portionwise to the solution over a period of 30 min, during which time a light-yellow precipitate of sulfur started to separate out, and the mixture was stirred for 2 h at room temperature. The rest of DIB (0.26 g, 0.80 mmol) was added again over a period of 30 min and stirring continued for 12 h to effect the complete precipitation of yellow sulfur. The orange-red filtrate, collected after removal of sulfur, was added to 500 mL of water and acidified with glacial acetic acid to afford a very fine yellow-orange precipitate of adpcH<sub>2</sub>. The yellow precipitate was filtered, washed with water, and dried overnight to obtain 0.2 g of the pure product. Yield: 95% from dithiocarbamate. The <sup>1</sup>H NMR spectrum was identical with that of adpcH<sub>2</sub> prepared using method 2.

**2,2'-Dimethyl-4,4'-azobis(phenylcyanamido)-0.1H<sub>2</sub>O, Me<sub>2</sub>adpcH<sub>2</sub>.** Method 1. Yield: 55%. Method 2. Yield: 97%. Method 3. Yield: 95%. Anal. Calcd for C<sub>16</sub>H<sub>14</sub>N<sub>6</sub>O<sub>0.1</sub>: C, 65.78; H, 4.90; N, 28.77. Found: C, 65.74; H, 4.86; N, 28.48. <sup>1</sup>H NMR (300 MHz, DMSO-*d*<sub>6</sub>): 10.54 (2H, s), 7.65 (2H, d), 6.96 (2H, s), 6.90 (2H, dd), 2.67 (6H, s). IR (KBr): ν(NCN) 2243 cm<sup>−1</sup>.

**Syntheses of Tl<sub>2</sub>[R<sub>2</sub>R'<sub>2</sub>adpc] Salts. Tl<sub>2</sub>[Me<sub>2</sub>adpc].** Me<sub>2</sub>adpcH<sub>2</sub> (0.25 g, 0.93 mmol) was dissolved in a boiling acetone/water mixture (2:1, 300 mL), and about 1 mL of triethylamine was added. An orange precipitate quickly formed upon the addition of a solution of thallium acetate (0.45 g, 1.86 mmol) in an acetone/water mixture (2:1, 50 mL). The resulting mixture was then boiled for an additional 5 min and slowly cooled at −20 °C. Filtration afforded a bright-red-orange microcrystalline solid, which was washed with a cold water/acetone mixture and dried overnight to obtain 0.46 g of pure Tl<sub>2</sub>[Me<sub>2</sub>adpc]. Yield: 71%. Anal. Calcd for C<sub>16</sub>H<sub>12</sub>N<sub>6</sub>Tl<sub>2</sub>: C, 27.55; H, 1.74; N, 12.06. Found: C, 27.48; H, 1.52; N, 11.91. <sup>1</sup>H NMR (300 MHz, DMSO-*d*<sub>6</sub>): 7.36 (2H, d), 6.49 (2H, s), 6.40 (2H, d), 2.45 (6H, s). IR (KBr): ν(NCN) 2083 and 2061 cm<sup>−1</sup>.

**Tl<sub>2</sub>[adpc].** This compound was prepared by following literature procedures.<sup>5</sup>

**Tl<sub>2</sub>[Cl<sub>2</sub>adpc].** This compound was prepared following the method used to prepare Tl<sub>2</sub>[Me<sub>2</sub>adpc]. Yield: 55%. Anal. Calcd for C<sub>14</sub>H<sub>8</sub>N<sub>6</sub>Tl<sub>2</sub>: C, 22.77; H, 0.82; N, 11.39. Found: C, 22.92; H, 1.19; N, 11.37. <sup>1</sup>H NMR (300 MHz, DMSO-*d*<sub>6</sub>): 7.55 (2H, d), 7.44 (2H, dd), 6.96 (2H, d). IR (KBr): ν(NCN) 2099 cm<sup>−1</sup>.

**Tl<sub>2</sub>[Cl<sub>4</sub>adpc].** Crude Tl<sub>2</sub>[Cl<sub>4</sub>adpc] was prepared following the method used for Tl<sub>2</sub>[Me<sub>2</sub>adpc]. <sup>1</sup>H NMR (300 MHz, DMSO-*d*<sub>6</sub>): 7.59 (2H, s), 6.95 (2H, s). IR (KBr): ν(NCN) 2115 cm<sup>−1</sup>. This salt did not give acceptable elemental analysis and was used as isolated.

**Preparation of [AsPh<sub>4</sub>]<sub>2</sub>[Me<sub>2</sub>adpc].** Me<sub>2</sub>adpcH<sub>2</sub> (0.10 g, 0.93 mmol) was dissolved in 50 mL of 2 M NaOH(aq). To this was added a solution of [AsPh<sub>4</sub>]Cl·H<sub>2</sub>O (0.35 g, 0.80 mmol) in 20 mL of water, and the mixture was stirred for 15 min. The red precipitate was collected and washed with 30 mL of water. Recrystallization from boiling acetonitrile gave red needle-shaped crystals of [AsPh<sub>4</sub>]<sub>2</sub>[Me<sub>2</sub>adpc] that were suitable for crystallographic analysis. Yield: 0.25 g, 60%. <sup>1</sup>H NMR (300 MHz, DMSO-*d*<sub>6</sub>): 7.36 (2H, d), 6.49 (2H, s), 6.40 (2H, d), 2.45 (6H, s). IR (KBr): ν(NCN) 2083 and 2061 cm<sup>−1</sup>.

**Syntheses of Complexes. [Ru(tpy)(bpy)]<sub>2</sub>(μ-Me<sub>2</sub>adpc)[PF<sub>6</sub>]<sub>2</sub>·H<sub>2</sub>O.** To a solution of Me<sub>2</sub>adpcH<sub>2</sub> (0.10 g, 0.314 mmol) in anhydrous DMF (90 mL) was added 2.5 M BuLi in hexane (0.3 mL, 0.698 mmol) under an inert atmosphere at −40 °C, and the mixture was stirred for 30 min at the same temperature. The resulting dark-red solution was then brought to room temperature, treated with [Ru(tpy)(bpy)Cl]·[PF<sub>6</sub>]<sub>2</sub> (0.42 g, 0.628 mmol) and TIPF<sub>6</sub> (0.22 g, 0.628 mmol), and refluxed under an inert atmosphere for 2 days. The resulting mixture

was chilled overnight at −20 °C and filtered to remove a fine white precipitate of TlCl. The dark-brown filtrate was rotaevaporated to dryness, redissolved in acetone (30 mL), and added to anhydrous ether (1 L) to precipitate 0.40 g of the crude product. The dinuclear complex was purified using an alumina column (grade III, Brockman acidic, 330 g) and toluene/acetonitrile and DMF as eluents. The first three bands containing starting materials and mononuclear impurities were eluted by 1:1, 1:2, and 1:3 toluene/acetonitrile. The fourth reddish-brown band was identified as the dinuclear complex and eluted with 1:1 DMF/acetonitrile. The resulting mass after removal of the solvent was redissolved in acetone (20 mL), filtered, and treated with anhydrous diethyl ether (300 mL) to precipitate the dark-brown product. Recrystallization of the complex from its saturated solution in DMF by slow diffusion of diethyl ether, followed by vacuum drying, afforded 0.20 g of the pure complex. Yield: 38%. Anal. Calcd for C<sub>68</sub>H<sub>56</sub>N<sub>16</sub>P<sub>2</sub>F<sub>12</sub>ORu<sub>2</sub>: C, 50.88; H, 3.52; N, 13.96. Found: C, 51.07; H, 3.87; N, 14.19. <sup>1</sup>H NMR (300 MHz, DMSO-*d*<sub>6</sub>): 9.68 (2H, d), 8.97 (2H, d), 8.92 (4H, d), 8.80 (4H, d), 8.70 (2H, d), 8.41 (2H, t), 8.33 (2H, t), 8.11 (6H, dd), 7.86 (2H, t), 7.75 (4H, d), 7.55–7.39 (6H, m), 7.20–7.13 (2H, m), 7.12 (2H, s), 5.61 (2H, s), 2.21 (6H, s), 1.80 (6H, s). IR (KBr): ν(NCN) 2152 cm<sup>−1</sup>.

**[Ru(tpy)(bpy)]<sub>2</sub>(μ-Me<sub>2</sub>adpc)[PF<sub>6</sub>]<sub>2</sub>·H<sub>2</sub>O.** A mixture of [Ru(tpy)(bpy)Cl][PF<sub>6</sub>]<sub>2</sub> (0.38 g, 0.56 mmol) and Tl<sub>2</sub>[Me<sub>2</sub>adpc] (0.20 g, 0.28 mmol) was refluxed in DMF (50 mL) for 48 h. The reaction mixture was then chilled at −20 °C and filtered through Celite to remove a fine white precipitate of TlCl. The dark-brown filtrate was then rotaevaporated to dryness to yield 0.51 g of the crude product, which after recrystallization from its saturated solution in DMF by slow diffusion of diethyl ether, followed by filtration and vacuum drying, gave 0.41 g of the pure dark-brown complex. Yield: 93%. Anal. Calcd for C<sub>66</sub>H<sub>52</sub>N<sub>16</sub>P<sub>2</sub>F<sub>12</sub>ORu<sub>2</sub>: C, 50.26; H, 3.32; N, 14.21. Found: C, 50.27; H, 3.13; N, 13.86. <sup>1</sup>H NMR (300 MHz, DMSO-*d*<sub>6</sub>): 9.69 (2H, d), 9.00 (2H, d), 8.94 (4H, d), 8.82 (4H, d), 8.73 (2H, d), 8.44 (2H, t), 8.35 (2H, t), 8.13 (6H, dd), 7.89 (2H, t), 7.77 (4H, d), 7.49 (6H, dd), 7.18 (4H, dd), 5.95 (2H, d), 5.87 (2H, s), 2.31 (6H, s). IR (KBr): ν(NCN) 2164 cm<sup>−1</sup>.

**[Ru(tpy)(bpy)]<sub>2</sub>(μ-adpc)[PF<sub>6</sub>]<sub>2</sub>.** This complex was prepared by following literature procedures.<sup>5</sup>

**[Ru(tpy)(bpy)]<sub>2</sub>(μ-Cl<sub>2</sub>adpc)[PF<sub>6</sub>]<sub>2</sub>·DMF.** A mixture of [Ru(tpy)(bpy)Cl][PF<sub>6</sub>]<sub>2</sub> (0.61 g, 0.91 mmol) and Tl<sub>2</sub>[Cl<sub>2</sub>adpc] (0.33 g, 0.45 mmol) in 100 mL of DMF was refluxed for 48 h. After removal of a fine white precipitate of TlCl, the dark-brown filtrate was concentrated to 20 mL and added to diethyl ether (600 mL) to precipitate the crude product (0.71 g). About 0.41 g of the crude product was then dissolved in 80 mL of 1:1 acetonitrile/toluene and purified by column chromatography using an alumina column (50 cm × 3 cm, grade III, Brockman acidic, 250 g). The first three bands containing starting materials and mononuclear impurities were eluted with 1:1 and 2:1 acetonitrile/toluene. The fourth dark-brown band containing the target compound was eluted with 3:1 acetonitrile/toluene, filtered, and evaporated to dryness to obtain the dark-brown solid. Recrystallization was achieved by slow diffusion of diethyl ether into a saturated solution of the complex in DMF (30 mL), which after filtration and vacuum drying gave 0.36 g of the pure dark-brown complex. Yield: 36%. Anal. Calcd for C<sub>67</sub>H<sub>51</sub>N<sub>17</sub>Cl<sub>2</sub>P<sub>2</sub>F<sub>12</sub>ORu<sub>2</sub>: C, 48.09; H, 3.07; N, 14.23. Found: C, 47.97; H, 3.45; N, 14.26. <sup>1</sup>H NMR (300 MHz, DMSO-*d*<sub>6</sub>): 9.67 (2H, d), 8.98 (2H, d), 8.93 (4H, d), 8.81 (4H, d), 8.72 (2H, d), 8.50–8.30 (4H, m), 8.12 (6H, m), 7.89 (2H, t), 7.76 (4H, d), 7.49 (6H, m), 7.24 (2H, dd), 7.18 (2H, t), 5.88 (2H, d). IR (KBr): ν(NCN) 2164 cm<sup>−1</sup>.

**[Ru(tpy)(bpy)]<sub>2</sub>(μ-Cl<sub>4</sub>adpc)[PF<sub>6</sub>]<sub>2</sub>·5H<sub>2</sub>O.** The complex was prepared by following the above procedure with some modification: A mixture of [Ru(tpy)(bpy)Cl] (0.58 g, 0.43 mmol) and crude Tl<sub>2</sub>[Cl<sub>4</sub>adpc] (0.35 g) was refluxed in DMF (130 mL) for 4 days to yield 0.69 g of the crude product. Column chromatography of 0.30 g of the crude product was performed using an alumina column (grade IV, Brockman acidic, 300 g). The fourth deep-purple band was eluted with pure acetonitrile and 10% methanol (in acetonitrile) to yield a dark-brown complex that lacks the [PF<sub>6</sub>]<sub>2</sub> anion [recognized by IR for ν(PF<sub>6</sub>): 842 cm<sup>−1</sup>]. This complex was then stirred in the boiling

mixture of DMF and water (1:1, 40 mL) in the presence of excess  $\text{NH}_4\text{PF}_6$  (5 equiv) for 10 min, and the resulting mixture was cooled to room temperature to obtain  $[\text{PF}_6]$  salt of the complex. The pure dark-brown complex (0.1 g) was obtained by slow diffusion of diethyl ether into a saturated solution of the complex in DMF. Yield: 13%. Anal. Calcd for  $\text{C}_{64}\text{H}_{52}\text{N}_{16}\text{Cl}_4\text{P}_2\text{F}_{12}\text{O}_3\text{Ru}_2$ : C, 43.70; H, 2.98; N, 12.74. Found: C, 43.85; H, 3.10; N, 13.00.  $^1\text{H}$  NMR (300 MHz,  $\text{DMSO}-d_6$ ): 9.64 (2H, d), 8.97 (2H, d), 8.93 (4H, d), 8.81 (4H, d), 8.71 (2H, d), 8.50–8.28 (4H, m), 8.12 (6H, m), 7.88 (2H, t), 7.76 (4H, d), 7.48 (6H, m), 7.43 (2H, s), 7.18 (2H, t), 5.88 (2H, s). IR (KBr):  $\nu(\text{NCN})$  2166  $\text{cm}^{-1}$ .

**Crystallography.** Diffraction data for a suitable crystal of  $[\text{AsPh}_4]_2[\text{Me}_2\text{adpc}]$  were collected on a 1K Siemens Smart CCD using Mo  $K\alpha$  radiation ( $\lambda = 0.71073 \text{ \AA}$ ) at 120(2) K using an  $\omega$ -scan technique and corrected for absorptions using equivalent reflections.

Unit cell parameters were obtained from 60 data frames,  $0.3^\circ \omega$ , from three different sections of the Ewald sphere. The systematic absences in the diffraction data are uniquely consistent with the reported space group. Direct methods were used to solve the structures, and refinement was done with full-matrix least-squares procedures. All non-hydrogen atoms were refined with anisotropic displacement parameters. All hydrogen atoms were treated as idealized contributions. Structure factors are contained in the *SHELXTL* 6.12 program library (Sheldrick, G. M. *Acta Crystallogr., Sect. A* **2008**, *64*, 112–122). Tables of crystallographic data and bond lengths and angles are given in the SI (Tables S1 and S2). The CIF has been deposited under CCDC 1026272.

## ■ ASSOCIATED CONTENT

### ● Supporting Information

Synthetic procedures of organic precursors and their  $^1\text{H}$  NMR spectra, figure showing the COSY NMR of  $[\{\text{Ru}(\text{tpy})\text{-}(\text{bpy})\}_2(\mu\text{-Me}_2\text{adpc})](\text{PF}_6)_2$ , three tables of NMR data of the complexes  $\text{R}_2\text{R}'_2\text{adpcH}_2$  and  $\text{Ti}_2[\text{R}_2\text{R}'_2\text{adpc}]$  salts, an ORTEP diagram of the  $\text{Me}_2\text{adpc}^{2-}$  and tetraphenylarsonium ions showing atomic labeling, six tables of crystallographic data and bond lengths, angles, and dihedral angles, and four spectra of IR and vis–NIR spectroelectrochemistry. This material is available free of charge via the Internet at <http://pubs.acs.org>.

## ■ AUTHOR INFORMATION

### Corresponding Author

\*E-mail: [robert\\_crutchley@carleton.ca](mailto:robert_crutchley@carleton.ca).

### Notes

The authors declare no competing financial interest.

## ■ ACKNOWLEDGMENTS

This work is supported by Carleton University and the Natural Sciences and Engineering Research Council of Canada. We thank Serge Gorelsky for attempting the DFT calculations of the  $[\{\text{Ru}(\text{tpy})(\text{bpy})\}_2(\mu\text{-adpc})]^{3+}$  ion.

## ■ REFERENCES

- (1) (a) Brunschwig, B. S.; Sutin, N. *Coord. Chem. Rev.* **1999**, *187*, 233. (b) Demadis, K. D.; Hartshorn, C. M.; Meyer, T. J. *Chem. Rev.* **2001**, *101*, 2655. (c) Endicott, J. F. *Coord. Chem. Rev.* **2005**, *249*, 343.
- (2) (a) Mosher, C. C. M.; Keske, J. M.; Warncke, K.; Farid, R. S.; Dutton, L. *Nature* **1992**, *355*, 796. (b) Gray, H. B.; Winkler, J. R. *Proc. Natl. Acad. Sci. U.S.A.* **2005**, *102*, 3534.
- (3) (a) Service, R. F. *Science* **2001**, *294*, 2442. (b) Martin, C. R.; Baker, L. A. *Science* **2005**, *305*, 67. (c) Lu, W.; Lieber, C. M. *Nat. Mater.* **2007**, *6*, 841.
- (4) Brunschwig, B. S.; Creutz, C.; Sutin, N. *Chem. Soc. Rev.* **2002**, *31*, 168.
- (5) Mosher, P. J.; Yap, G. P. A.; Crutchley, R. J. *Inorg. Chem.* **2001**, *40*, 1189.

- (6) Al-Noaimi, M.; Yap, G. P. A.; Crutchley, R. J. *Inorg. Chem.* **2004**, *43*, 1770.
- (7) Robin, M. B.; Day, P. *Adv. Inorg. Chem. Radiochem.* **1967**, *10*, 247.
- (8) Chisholm, M. H.; D'Acchioli, J. S.; Hadad, C. M.; Patmore, N. J. *Inorg. Chem.* **2006**, *45*, 11035.
- (9) (a) Lever, A. B. P. *Coord. Chem. Rev.* **2010**, *254*, 1397–1405. (b) Kaim, W.; Schwederski, B. *Coord. Chem. Rev.* **2010**, *254*, 1580.
- (10) Naklicki, M. L.; Gorelsky, S. I.; Kaim, W.; Sarkar, B.; Crutchley, R. J. *Inorg. Chem.* **2012**, *51*, 1400.
- (11) Mosher, P. J.; Yap, G. P. A.; Crutchley, R. J. *Inorg. Chem.* **2001**, *40*, 550.
- (12) Gerson, F.; Gescheidt, G.; Möckel, R.; Aumüller, A.; Erk, P.; Hünig, S. *Helv. Chim. Acta* **1988**, *71*, 1665.
- (13) Choudhuri, M. M. R.; Kaim, W.; Sarkar, B.; Crutchley, R. J. *Inorg. Chem.* **2013**, *52*, 11060.
- (14) (a) Kasack, V.; Kaim, W.; Binder, J.; Jordanov, J.; Roth, E. *Inorg. Chem.* **1995**, *34*, 1924. (b) Ernst, S.; Hänel, P.; Jordanov, J.; Kaim, W.; Kasack, V.; Roth, E. *J. Am. Chem. Soc.* **1989**, *111*, 1733.
- (15) Remenyi, C.; Kaupp, M. *J. Am. Chem. Soc.* **2005**, *127*, 11399.
- (16) Kurzer, F.; Douraghi-Zadeh, K. *Chem. Rev.* **1967**, *67*, 107.
- (17) Crutchley, R. J.; McCaw, K.; Lee, F. L.; Gabe, E. J. *Inorg. Chem.* **1990**, *29*, 2576.
- (18) DeRosa, M. C.; White, C. A.; Evans, C. E. B.; Crutchley, R. J. *J. Am. Chem. Soc.* **2001**, *123*, 1396.
- (19) (a) Best, S. P.; Clark, R. J. H.; McQueen, R. C. S.; Joss, S. J. *Am. Chem. Soc.* **1989**, *111*, 548. (b) Crutchley, R. J. *Angew. Chem., Int. Ed.* **2005**, *44*, 6452.
- (20) Hadda, T. B.; Bozec, H. L. *Inorg. Chim. Acta* **1993**, *204*, 103.
- (21) Takeuchi, K. J.; Thompson, M. S.; Pipes, D. W.; Meyer, T. J. *Inorg. Chem.* **1984**, *23*, 1845.
- (22) Gennett, T.; Milner, D. F.; Weaver, M. J. *J. Phys. Chem.* **1985**, *89*, 2787.
- (23) (a) Krejčík, M.; Danek, M.; Hartl, F. J. *Electroanal. Chem.* **1991**, *317*, 179. (b) Evans, C. E. B.; Yap, G. P. A.; Crutchley, R. J. *Inorg. Chem.* **1998**, *37*, 6161. (b) Evans, C. E. B. Ph.D. Thesis, Carleton University, Ottawa, Canada, 1997.